



ELSEVIER

Available online at www.sciencedirect.com

 ScienceDirect

Proceedings of the Combustion Institute 31 (2007) 2239–2246

Proceedings
of the
Combustion
Institute

www.elsevier.com/locate/proci

Liquid fuel microcombustor using microfabricated multiplexed electrospray sources

Weiwei Deng ^a, James F. Klemic ^b, Xiaohui Li ^b,
Mark A. Reed ^b, Alessandro Gomez ^{a,*}

^a Department of Mechanical Engineering, Yale Center for Combustion Studies, New Haven, CT 06520, USA

^b Department of Electrical Engineering Yale University, New Haven, CT 06520, USA

Abstract

The use of hydrocarbons is very appealing for the realization of high energy density power sources, so long as the fuel can be stored in the liquid phase. As a result, except for the most volatile hydrocarbons, a miniaturized combustor must rely on a good design of the fuel atomizer, which should yield small, rapidly evaporating droplets to generate the fuel vapor promptly, mix it with the oxidizer and subsequently burn it with the attending heat release. To achieve this goal, we relied on the use of multiplexed electrosprays and a catalytic reactor for fuel conversion consisting of a pack of catalyst impregnated meshes (Microliths[®]). Fuel dispersion was achieved by microfabricating the fuel distributor in Si using deep reactive ion etching. Tests were performed using JP-8 as the liquid fuel. Preliminary experiments in a 0.8 cm³ optically accessible combustor, enabling the measurements of droplet size and velocity, revealed that the spreading of the electrospray by Coulombic repulsion is the phenomenon controlling the volume of the mixing/evaporation chamber. Droplet evaporation occurs in the thin (Peclet number dependent) thermal layer preceding the catalytic section of the combustor. Subsequent system optimization in a fully ceramic combustor yielded a volumetric heat release rate as large as 270 MW/m³, a value that is of the same order as that of conventional gas turbines. The small overall combustor volume, at only 0.22 cm³, suggests that the large volumetric energy density was achieved despite the device large surface-to-volume ratio and attending heat losses. The fuel was fully oxidized, with CO/CO₂ ratios well under 1% over a range of equivalence ratios. Inspection of the combustor inner walls after operating continuously for 10 h, revealed no traces of deposits. The design has the potential of being scaled either up or down, depending on power needs.

© 2006 The Combustion Institute. Published by Elsevier Inc. All rights reserved.

Keywords: Electrospray; Catalytic combustion; Microfabrication; Portable power; Microcombustion; Microfluidics

1. Introduction

Liquid hydrocarbons are known to have a much higher energy density than conventional

batteries (e.g., 42 MJ/kg for a typical hydrocarbon versus 0.6 MJ/kg for a Li-Ion battery). For this reason, the realization of liquid fueled batteries, that is, of portable electricity generators operating on liquid fuels, may result in dramatic improvements on the state-of-the-art, even when the overall energy conversion efficiency is modest. This outcome would be particularly important

* Corresponding author. Fax: +1 203 432 7654.
E-mail address: alessandro.gomez@yale.edu (A. Gomez).

when space and mass are at a premium. For example, for the past several years there has been a DARPA program aimed at developing small scale liquid fuel based energy converters for military applications. Several papers were presented at the last two Symposia, advocating different technologies for the realization of this goal. A review was presented in [1], covering fundamentals and potential applications, and a colloquium was dedicated to the topic in the present Symposium.

Systems can be classified either in terms of size or conversion principle. With respect to size, a distinction can be made between systems at the microscale, with overall dimensions on the order of at most a few centimeters, but with features that are resolved at submillimeter scale, and mesoscale systems. The latter would have overall dimensions on the order of perhaps a few tens of centimeters, which is still small by comparison with typical heat engines. Energy conversion is based on cycles involving moving parts, as is the case for a miniaturized gas turbine [2], a Wankel engine [3], and a variety of free-piston systems [4], including Stirling systems [5]. Also considered are direct energy conversion alternatives using, for example, thermoelectric generation, with no moving parts, except for those associated with fluid pumping [6,7].

At the mesoscale the challenges are significant because of the increase in surface-to-volume ratio of these devices, as compared to more typical engineering systems and the reduced residence time in the reacting environment. Nevertheless, there are no fundamental impediments to scale down well-established engineering cycles to this scale, albeit at a reduced efficiency because of the inevitable increase in losses. At the microscale, on the other hand, the challenges can be prohibitive, since losses may overwhelm the energy release with ensuing quenching of the chemical reactions that yields the energy conversion. Furthermore, any energy conversion cycle will require the separation of the hot zone from the cold region to maintain good thermodynamic efficiency. This task poses significant heat management problems in general, and at the microscale in particular.

Regardless of the scale of the problem and of the energy conversion technique, the starting fuel must be in the liquid phase since the energy density gain can be realized only if the chemical energy is also in a dense phase. This consideration makes the all too common choice of hydrogen in feasibility demonstrations inapplicable, since it is difficult to store and transport in the liquid phase because of the weight penalty of the necessary cryogenic tank. Other potential fuels are either alcohols or hydrocarbons that are stored in the liquid phase. Among the hydrocarbons, propane and butane are the simplest choices because of their high

volatility, which enables storage in the liquid phase and burning in the gas phase without the need for any atomization or vaporization device. Alcohols are perhaps less than ideal since they have lower heating values as compared to hydrocarbons and a larger energetic penalty would have to be paid for their vaporization. Thus, liquid hydrocarbons remain the preferred energetic choice.

Heat release from a liquid fuel in a premixed configuration necessarily starts with the fuel vaporization, followed by mixing with the oxidizer and ultimately chemical reaction. Complete conversion in a miniaturized system will benefit from catalytic conversion, especially under conditions of large surface-to-volume ratios. A catalytically coated surface would, in fact, play an active role in fuel conversion, as opposed to providing a loss mechanism that would hinder the fuel oxidation.

For these reasons, our group has been working on the realization of small scale combustors using a combination of direct fuel injection by electro-spray dispersion, premixing of fuel and air and catalytic fuel conversion, as documented in [5,8,9]. The liquid of choice is JP-8, a jet fuel that poses notorious challenges for clean burning, including fouling and soot. Clean and efficient burning was demonstrated in a system that was miniaturized at a volumetric power density of at most 30 MW/m³. If we compare this figure with that typical of gas turbines, that is on the order of 200–400 MW/m³, the system exhibits a volumetric energy density one order of magnitude smaller.

For a relatively nonvolatile fuel like JP-8, fuel vaporization and mixing with the oxidizer may control the combustor dimension, especially in a reactor in which catalysts are used to accelerate the fuel oxidation, as in the present design. With this premise, intervening on the fuel atomization and dispersion may yield the most significant payoff. In [5,9], fuel atomization was achieved by dispersing the fluid in electrospays using an atomizer built by conventional machining. With the advent of microfabrication, adapting conventional silicon integrated circuit microlithographic fabrication technology to the machining of mechanical structures in silicon and other materials [10,11], there is an opportunity to optimize the fuel injector to yield smaller and rapidly evaporating droplets, which may ultimately lead to the realization of a much smaller combustor. In addition, microlithography offers an economy of scale in terms of device complexity: within the constraints of a specific microlithographic fabrication process, one may realize arbitrarily complex devices without additional fabrication steps. We report here on a novel fuel dispersion technique based on the use of such a microfabricated fuel atomizer, enabling the multiplexing of fuel electrospays and subsequent burning in a very compact configuration.

2. The electro spray and microcombustion

The electro spray is ideally suited for the development of microscale atomizers for liquid fuel combustors since it is one of the few devices that can disperse the low flow rates that are required in miniaturized combustors. A particular type of electro spray is under consideration that is characterized by the critical feature of a tight control of the size distribution of the resulting aerosol. Such a system can be implemented by feeding a liquid with sufficient electric conductivity through a small nozzle, maintained at a few kilovolts relative to a ground electrode positioned at an appropriate distance from it. The liquid meniscus at the outlet of the capillary takes a conical shape under the action of the electric field, with a thin jet emerging from the cone tip. This jet breaks up further downstream into a spray of fine, charged droplets. Because of the morphology of the liquid meniscus, this regime is labeled as the cone-jet mode [12]. Among the key features distinguishing the cone-jet electro spray from other atomization techniques are: quasi-monodispersity of the droplets with relative standard deviation on the order of 10% and Coulombic repulsion of the charged droplets, which induces spray self-dispersion, prevents droplet coalescence and enhances mixing with the oxidizer stream. Since the electro spray exhibits a monotonic dependence of droplet size on flow rate, if small droplets are needed for fast evaporation or better dispersion, mass flow rate may be minuscule even by the standard of small scale combustors. As a result even in this case, multiplexing the spray source is necessary. Figure 1 shows the relation between liquid flow rate and droplet size as measured by a fiber optic Phase Doppler System (TSI, Inc.) with the system operating in the single cone-jet mode. In particular, for JP-8 the power law dependence is roughly $D \propto \dot{Q}^{0.5}$. For example, the size corresponding to a target flow rate of, say, 6 cc/h, which would

yield 60 W_t of chemical power, is a rather large 41 μm. If the total JP-8 flow rate is partitioned in n electro sprays, the droplet size at the injection is reduced by a factor $n^{0.5}$, and the droplet evaporation time, which scales with the square of the droplet diameter, would be reduced by a factor of n . Furthermore, the large charge-to-mass ratio of small droplets would yield better dispersion and mixing with the oxidizer. Both of these effects would ensure that the partitioning the total flow rate into a multitude of jets operating in parallel results in a reduction of the dimensions of the vaporization/mixing chamber, as compared to dispersing the fluid with a single electro spray.

3. Microfabrication

A multiplexed electro spray distributor was microfabricated using Deep Reactive Ion Etch (DRIE) of silicon wafers. Uniform nozzles, interspaced at a distance of 0.675 mm, and protruding 0.450 mm were patterned with an outer diameter of 0.220 mm, and an inner diameter of 0.120 mm. Using double-sided wafer processing and deep reactive ion etching, a polished Si wafer with an oxide mask layer was patterned on both sides to realize nozzle arrays. DRIE of silicon can yield essentially straight sidewalls with large aspect ratios. The inset in Fig. 2 below shows a scanning electron micrograph including several nozzles. Since the minimum feature sizes can be on the order of 1 μm, the approach guarantees virtually identical protrusions, all acting as pseudo-capillaries. The reproducibility of geometric features between protrusions is an important prerequisite to equidistribution of flow rates among the multiplexed nozzles, and to the establishment of a controlled electric field at each nozzle.

4. Electrode configuration and burner assembly

The realization of the microfabricated distributor is only the first step. The selection of the electrode configuration is crucial contrary to the case of operation with a single electro spray that can be established with a variety of electrode geometries. To establish an intense electric field, the simplest configuration would entail mounting a flat electrode at a distance from the multiplexed distributor. The distance selection is critical, since a few characteristic length scales are already apparent in the distributor design: the inter-nozzle distance, l_{in} , the nozzle protrusion, h and the nozzle diameter, D . Microfabrication allows for the manufacturing of essentially planar structures, with protrusions limited by the wafer thickness. In the present system, h was limited to 0.45 mm, which is of the same order as the inter-nozzle distance, l_{in} , at 0.675 mm. If the flat electrode is mounted

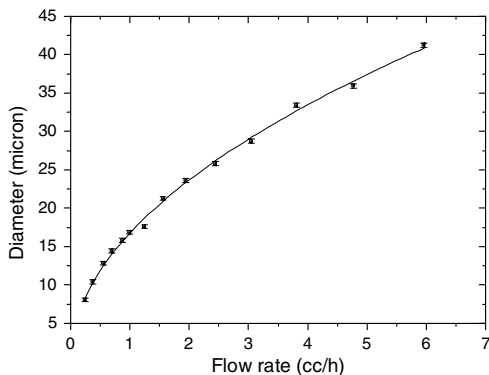


Fig. 1. Average droplet diameter as a function of flow rate for a single JP-8 electro spray in the cone-jet regime.

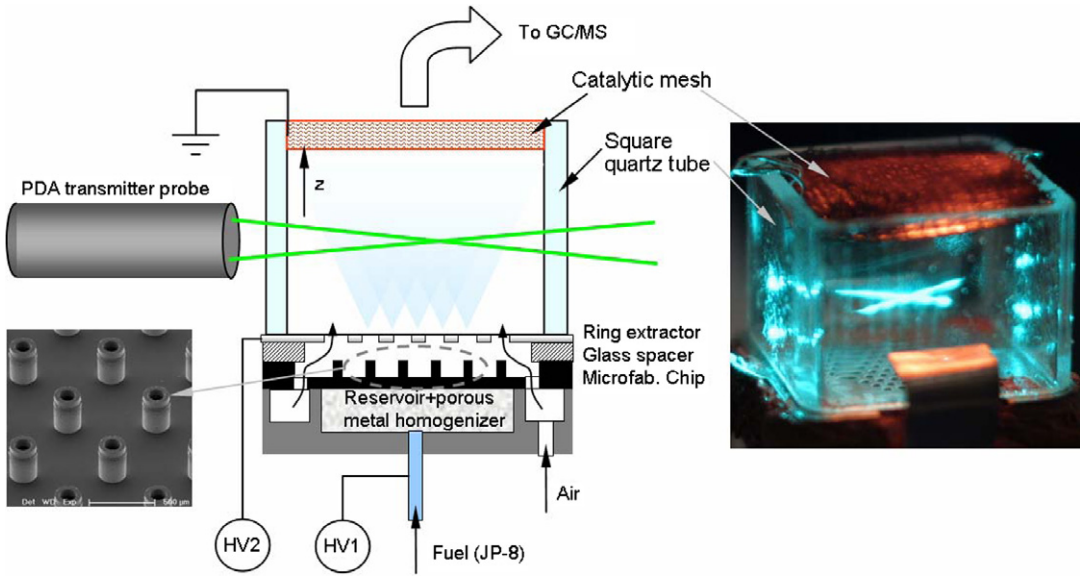


Fig. 2. (Left) Schematic of the experimental system, with inset showing a SEM micrograph of some microfabricated nozzles. (Right) Optically accessible miniaturized burner in operation.

at a distance $L \gg h$, the effect of the protrusion would be irrelevant and the electric field established would essentially be that which is between two capacitor plates. With such a configuration, sufficiently intense electric fields cannot be established for the cone-jet mode of operation before the onset of corona breakdown in the surrounding gas. Furthermore, feedback from space charge may become inevitable. If, on the other hand, $L \sim h \ll l_{in}$, the effect of the protrusions will be significant and the field can be localized with minimal influence of the neighboring nozzles. Inevitable flooding of the liquid flowing through the system would prevent operation with a ground electrode a fraction of a millimeter away from the nozzle. If a ring electrode to let the fluid through a small opening is used, the cone-jet can be established and a spray with the right “quality” can be formed. This configuration, often called *extractor electrode* is typically used in electron beam applications. It was also used in early electrospray applications to electric propulsion (e.g., [13]) and combustion (e.g., [14]). Without additional electro-optics the generated droplets would eventually reverse their paths and be attracted back to the lower potential electrode, causing flooding and eventual interruption of the flow. An additional electrode placed downstream at a lower potential effectively “sweeps” the droplets away for use in the intended applications. This can also be combined with an external flow that would drag the droplet away overcoming electrostatic attractive forces. The additional advantage of this configuration is that it shields the cone-jet region at the source of the spray from the region

where the spray cloud disperses, with attending space charge. A separation of the cone-jet region from the spray utilization region is generally desirable for stability and combustion applications.

The chosen electrode configuration is depicted in the schematic in Fig. 2. The microfabricated Si distributor is charged at about 2 KV potential above that of a metal ring extractor plate positioned at a distance of typically 0.525 mm by means of a glass insulator/spacer, under conditions in which $L < h < l_{in}$. Since L is not much smaller than l_{in} , it is likely that nozzle cross talk is not completely eliminated [15]. The stainless steel ring extractor itself was designed and microfabricated using photolithography and metal etching to tolerances compatible with the microfabricated nozzle array. Visible in the schematic is a ground electrode several millimeters downstream. A catalytic reactor consisting of a pack of catalyst impregnated meshes (PCI, North Haven, CT, USA), as in our earlier work [8,9], had the dual function of acting as the ground electrode and complete the fuel oxidation.

A typical testing arrangement requires mounting the microfabricated distributor on a liquid reservoir, positioning the additional electrodes, and providing an electric connection to maintain the desired voltage drop between the distributor and the other electrodes. Although the multiplexed system consists of 91 nozzles, to simplify the prototype testing, only 19 nozzles were operated, while the others were plugged up with an epoxy to prevent flow. The nozzle density was approximately 250 nozzles/cm². A quartz chimney was mounted above the distributor/electrode combination.

It had a square cross section to provide optical access for debugging the combustor performance. It also enabled the application of Phase Doppler Anemometry to measure droplet size and velocity. The electro spray set-up was mounted on a multi-direction translational stage allowing for the systematic scanning of the spray by the laser probe volume. For each measurement, 5000 counts per sample were taken. Thermocouple measurements were performed at discrete locations, compatibly with the constraints of the small geometry. All tests were performed using JP-8 doped with 0.3% of Stadis 450 to enhance its electric conductivity to a value of $4.5 \times 10^{-9} \text{ } \Omega\text{cm}$, and allow for the establishment of cone-jet electro sprays. The liquid was pumped continuously into the reservoir using a syringe pump. Air was admitted through a special passage in the fuel reservoir and entered the mixing chamber through the extractor ring. As a result, it is expected that air was homogeneously flowing through the entire burner cross-section, except for possible recirculation pockets in the chimney corners. The fuel flow rate was 6 cc/h. Air flow rates were varied to operate at equivalence ratio ranging from 0.3 to 0.6. To check for the completeness of the fuel conversion, gas samples were periodically drawn with a gas-tight syringe and analyzed off-line for CO and CO₂ concentrations, using a GC-MS (VARIAN CP-3800). Figure 2 (right) shows a picture of the system in operation.

5. Atomizer and burner performance

Figure 3 shows the droplet average diameter measured in an optimized system in a typical scan across an hexagonally patterned nozzle array with nozzle numbers identified in the inset in the figure. So long as the flow homogenizer, essentially a fine porous metal disk embedded in the liquid reser-

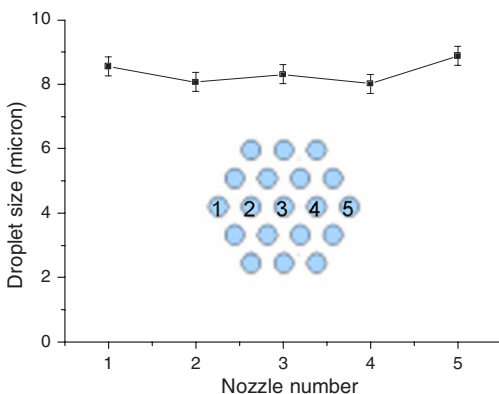


Fig. 3. Average droplet diameter in individual cone-jet electro sprays in the multiplexed mode.

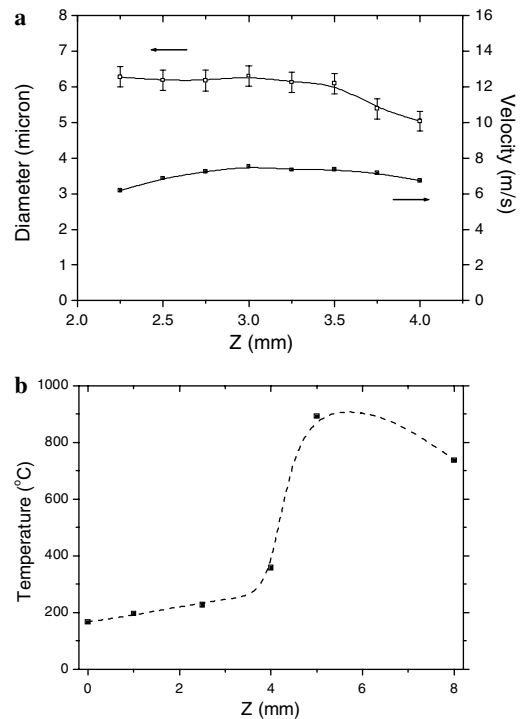


Fig. 4. Evolution of (a) average droplet diameter (left ordinate) and average droplet velocity (right ordinate) for a prototypical electro spray of the parallelized system, and (b) gaseous temperature as a function of the distance from the extractor electrode.

voir, distributes uniformly the liquid flow rate among the parallel nozzles, little variation in mean droplet size is found from nozzle to nozzle.

Figure 4a shows the average droplet size (left ordinate) and velocity (right ordinate) versus distance from the extractor electrode. The data track the evolution of a single spray, but, in view of Fig. 3, they also apply to all other sprays. Figure 4b shows the measured temperature as a function of the same spatial coordinate. For these measurements, the burner was operated at a fuel flow rate of 6 cc/h, an air flow rate of 1.84 L/min and an overall equivalence ratio of 0.5. In the first 5 mm above the extractor electrode, the parallel electro sprays could spread out by Coulombic repulsion and the fuel could mix with the air flow. The fuel/air mixture entered the catalytic reactor approximately at $z = 5 \text{ mm}$. The fuel conversion was completed at $z = 8 \text{ mm}$, after the flow had passed through a system of several catalytic meshes. The thickness of catalytic reactor was chosen on a trial and error basis, namely by adding more layers of catalytic meshes until a satisfactorily low emission was measured. A mirror allowed for visualization of the first mesh in the pack, which appeared to glow with good uniformity over a

Table 1
Relevant characteristic times as defined in the text

	τ_{ov}	τ_{ht}	τ_{ev}	τ_{st}	τ_{cat}
(ms)	0.7	0.14	0.1	1.8	0.43

circular area of about 9 mm in diameter. An examination of Fig. 4 shows that initially the droplet evaporation is modest, as a result of the “cold” temperature in the system. At the prevailing Peclet number, heat diffusion upstream is hampered by the opposed convective flow [16]. As a result the high temperature region is confined to a thermal layer with a thickness on the order of 1 mm. The only preheating upstream of this layer results from radiative feedback from the catalyst screen, estimated at 5 W and conduction through the chimney wall. Substantial droplet evaporation begins at $z = 3.5$ mm and continues in this thin thermal layer. The velocity of the droplets is reasonably uniform in the probed region at an average value of 7 m/s, as a result of the balance of electric force acting on the charged droplet and drag in the host gas. The temperature peaks at the first catalyst meshes and it drops off subsequently as less and less fuel conversion is achieved and the meshes passively cool off the gaseous stream.

On the basis of these measurements, it would appear that nearly half of the burner volume is effectively unused with little ongoing evaporation. This is not the case. This characteristic length is necessary to allow for the spreading of the sprays before evaporation takes off in the remaining path preceding the catalyst bed. An estimate of the characteristic times of the process is reported in Table 1. The relevant times are: τ_{ov} , the overall droplet residence time upstream of the catalyst bed; τ_{ht} , the droplet residence time in the high temperature thermal layer immediately preceding the catalytic reactor; τ_{ev} , the droplet evaporation time in the high temperature region; τ_{st} , the droplet stopping time; and τ_{cat} , the gas residence time in the catalytic reactor. Their values are 0.7, 0.14, 0.1, 1.8, and 0.43 ms, respectively. The following conclusions can be drawn from these estimates:

(a) The evaporation in the high temperature layer occurs very rapidly. Broadening of this layer, to bring the high temperature region closer to the extractor electrode would require decreasing the average velocity in the combustor. The thickness of this layer is, in fact, inversely dependent on the Peclet number. For a given burning rate, this goal can be achieved by either: (1) spacing the nozzles further apart and increasing the combustor cross-section, or (2) by varying the thermal diffusivity of the oxidizer. The second option would require synthetic air, with, for example He

replacing N_2 . The first option is unlikely to modify the overall evaporation/mixing volume because of the increased burner dimension in the transverse direction.

- (b) Little action seems to be taking place in the region immediately downstream of the extractor electrode with the notable exception of the spreading of the sprays by Coulombic repulsion. An estimate of the average inter-droplet distance can be gauged from the inverse cubic route of the droplet number density. From a peak value of 0.13 mm in the scan closest to the extractor plate, the average inter-droplet distance increases to 0.35 mm in the scan closest to the catalyst. To improve this spreading, and the ensuing enhancement of mixing with the oxidizer, it is advantageous to produce smaller droplets, which have higher charge-to-mass ratio [17], and, as a result, higher mobility as compared to large droplets. This, in turn, suggests that increasing multiplexing level, with the passage of even smaller flow rates per nozzle, would be beneficial. Additionally, a change in the ground electrode geometry, by floating the catalyst mesh and using an annular ground electrode, may also help the spreading of the electrospray.
- (c) A comparison of the overall droplet residence time and the droplet stopping time reveals that there is little room for using viscous drag to decelerate the droplets. Rather, it would be advantageous to modify the electric field between electrodes and provide an electrostatic decelerating force.
- (d) Despite the short overall residence time of the droplets, the mixing/evaporation section of the combustor occupies the majority (63%) of the volume, in view of the relative large velocity of the droplets.

Having optical access to the combustor was helpful in quantifying some of the characteristic times of the process. It also suggested means to further the system miniaturization. For example, the Coulombic expansion of the parallelized electrosprays suggests a truncated cone as an optimally small evaporator/mixing chamber. Also, realization of the structure in ceramic materials will reduce heat losses and help the droplet evaporation. As a result, the length of this region may be reduced below the 5 mm of the previously discussed experiments. To implement these improvements, we replaced the quartz chimney with a ceramic section shaped as a truncated cone, with inlet and outlet measuring 4 and 8 mm in diameter, respectively, and with a height of 4.2 mm. On top of the chimney, several layers of catalytic mesh were held in place by a ceramic holder. Each layer of the catalytic mesh was cut to a 8 mm diameter disc. As a result of these changes, the total volume of the burner was ~ 0.22 cm³, including that of the

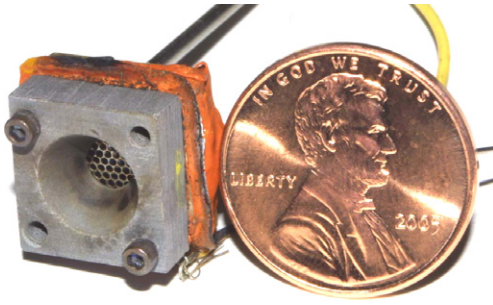


Fig. 5. Miniaturized ceramic burner.

catalytic reactor. Figure 5 shows the ceramic chimney bonded to the fuel distributor. The burner was tested in the fuel flow rate range of 3 to 6 cc/h with a fixed equivalence ratio of 0.5, corresponding to a power density as large as 270 MW/m^3 . This value is one order of magnitude larger than in [5] and of the same order as that typical of gas turbines ($200\text{--}400 \text{ MW/m}^3$). This result is particularly significant in the light of the dramatic miniaturization of the present set up, since a large surface-to-volume ratio should have been conducive to large heat losses.

Miniaturization with incomplete combustion may be a pyrrhic victory and the two goals of smallest combustor and complete combustion are often difficult to reconcile [18]. Fortunately, catalytic fuel conversion came to the rescue ensuring that even in this very small combustor the ratio of CO/CO_2 was kept at less than 3×10^{-3} throughout the range of investigated flow rates, as shown in Table 2.

The microfabricated fuel distributor can be readily scaled either up or down, depending on the power needs. Using microlithographic fabrication, one may multiplex by several orders of magnitudes using the same nozzle density and identical fabrication process. For example, maintaining the same packing density, but applying the mask to an entire wafer, with a diameter of approximately 10 cm, would yield the realization of 2.0×10^4 parallel sources in a relatively small footprint. This consideration suggests combustion applications that are not necessarily confined only to small scale. For example, flow rates on the order of 1000 cc/hr, corresponding to 10 kW, can be accommodated on a microfabricated distributor with a footprint of 8 cm^2 at the current nozzle density of 250 nozzles/ cm^2 , which is comparable to the cross-section of a cylinder of a typical IC engine.

Table 2

CO/CO_2 ratio as measured by GC/MS analysis of exhaust gases

$\dot{Q}_{\text{JP-8}}$ (cc/h)	3	4	5	6
$\text{CO}/\text{CO}_2(\%)$	0.22	0.07	0.15	0.3

6. Conclusions

The development of a miniaturized ceramic combustor operating on a jet fuel (JP-8) is described with the capability of achieving a volumetric heat release rate as large as 270 MW/m^3 . This result is particularly significant since this value is of the same order as that of conventional gas turbines, yet the overall combustor volume is only 0.22 cm^3 , which implies a much larger surface-to-volume ratio and, in principle, much larger heat losses. A cornerstone of the miniaturization is the microfabrication of a fuel atomizer consisting of several sub-millimeter nozzles, each anchoring an electrospray operating in the cone-jet mode. After droplet evaporation and subsequent mixing with the oxidizer stream, the mixture was fully oxidized in a catalytic reactor yielding CO/CO_2 ratios well under 1%. Measurements in an optically accessible combustor of 0.8 cm^3 revealed that 63% of the volume was necessary to vaporize the fuel and mix it with the oxidizer, the remainder being devoted to the catalytic fuel conversion. At the typical flow rates of 6 cc/h, with droplet sizes on the order of $7 \mu\text{m}$ in diameter, vaporization was nearly instantaneous at the average 800 K in the thermal layer preceding the catalyst. The physical effect controlling the mixing/evaporation volume was the dispersion of the parallelized electrosprays by Coulombic repulsion of the charged droplets.

Acknowledgments

We acknowledge the help of Dr. Subir Roychoudhuri from Precision Combustion Inc., who supplied the catalyst meshes (Microliths[®]), Mr. Nick Bernardo and Dr. Barbara La Mantia, who manufactured some parts for the testing of the microfabricated distributors and helped with the GC/MS sampling, respectively. The microfabrication was performed in part at the Cornell Nanoscale Science and Technology Facility (CNF), a member of the National Nanotechnology Infrastructure Network, which is supported by the National Science Foundation (Grant ECS 03-35765). The support of DARPA under Grant No. DAAD19-01-1-0664 (Dr. Richard J. Paur, Contract Monitor) and of the US Army under Grant No. W911NF-05-2-0015 (Mr. Bruce Geil, Contract Monitor) is gratefully acknowledged.

References

- [1] A.C. Fernandez-Pello, *Proc. Combust. Inst.* 29 (2002) 883–889.
- [2] A. Mehra, X. Zhang, A.A. Ayon, I.A. Waitz, M.A. Schmidt, C.M. Spadaccini, *J. MEMS* 9 (2000) 517–527.

- [3] Available at <http://www.me.berkeley.edu/mrcf/why.html>.
- [4] M. Kirtas, M. Disseau, D. Scarborough, J. Jagoda, S. Menon, *Proc. Combust. Inst.* 29 (2002) 917–925.
- [5] A. Gomez, J.J. Berry, S. Roychoudhury, B. Coriton, J. Huth, *Proc. Combust. Inst.* 31 (2007) 3251–3259.
- [6] J. Vican, B.F. Gajdeczko, F.L. Dryer, D.L. Milius, I.A. Aksay, R.A. Yetter, *Proc. Combust. Inst.* 29 (2002) 909–916.
- [7] F.J. Weinberg, D.M. Rowe, G. Min, P.D. Ronney, *Proc. Combust. Inst.* 29 (2002) 941–947.
- [8] D.C. Kyritsis, I. Guerrero-Arias, S. Roychoudhury, A. Gomez, *Proc. Combust. Inst.* 29 (2002) 965–972.
- [9] D.C. Kyritsis, B. Coriton, F. Faure, S. Roychoudhury, A. Gomez, *Combust. Flame* 139 (2004) 77–89.
- [10] M. Elwenspoek, H.V. Jansen, *Silicon Micromachining*, Cambridge University Press, London, 1999.
- [11] M. Madou, *Fundamentals of Microfabrication*, CRC Press, Boca Raton, Florida, 1997.
- [12] M. Cloupeau, B. Prunet-Foch, *J. Electrostat.* 22 (1989) 135–159.
- [13] C.D. Hendricks, *J. Coll. Sci.* 17 (1962) 249–259.
- [14] G. Chen, A. Gomez, *Combust. Sci. Technol.* 115 (1996) 177.
- [15] W. Deng, J.F. Klemic, X. Li, M.A. Reed, A. Gomez, *J. Aerosol Sci.* 37 (2006) 696–714.
- [16] M. Vera, A. Liñán, *Combust. Theory Model.* 8 (2004) 97–121.
- [17] K. Tang, A. Gomez, *Phys. Fluids A* 6 (1994) 2317–2332.
- [18] T.T. Leach, C.P. Cadou, *Proc. Combust. Inst.* 30 (2005) 2345–2437.